Determination of the dissolution kinetics of halite particles in mineral water during transition flow in batch systems

S.C. MAGALHÃES [1], T.F. FONSECA[1], M. DEMAUIR[1], L.A. CALÇADA[1] and C.M. SCHEID[1]

[1]Federal Rural University of Rio de Janeiro, Institute of Technology, Chemical Engineering Department. BR-467, Km 7, Campus of UFRRJ, Postal Code (CEP): 23.890-000, Seropedica, Rio de Janeiro, Brazil.
e-mail: scheid@ufrrj.br

Abstract

The aim of this work was to study the effect of the temperature and Reynolds number in halite salt particle dissolution in a stirred tank. The sample of salt was considered to be a population of particles of different sizes and of random geometry. We tried many of the correlations found in literature attempting to model the dissolution kinetics, but none corresponded to the experimental data obtained. We take from this evidence, that new correlations are necessary. To validate the model, a direct comparison between the experimental and calculated data was done, demonstrating that both results, with deviances of up to 15%, agree.

1. Introduction

The petroleum industry is facing technical difficulties in transposing the mineral salt layer located right above reservoirs. Some of these layers extend to a depth of 2000 meters. The main difficulty occurs when the salt particulate, a product of the drill destroying geological formations, invades the annular region between the wall of the well and the external diameter of the drill column. This particulate naturally dissolves in the drilling fluid, causing such operational problems as increasing the fluid's density and changing its viscosity. Besides, it is intended to drill dissolving the wall, as it has a natural tendency to jam the drill column due its plastic characteristics at a particular pressure and temperature.

Studies found in the literature are directed at studying the dynamic dissolution of mineral salts. The models are usually based on the macroscopic flux of mass, where it's always necessary to know the mass transfer coefficient. This coefficient is key because it represents the kinetic of the dissolution, also referred to as the mass liberation rate ([1] Aksel`rud, *et al.* 1992).

To validate the mathematical correlations, one should refer to experimental data, which must agree with the theoretical values. The literature offers possible methods; one widely employed is the rotating disk method ([2] Alkattan *et. al.* 1997). Although this method is used so as to simulate natural and industrial processes, it often bears no similarity to them. Hence, we propose an experimental system that bears a greater similarity to the real process occurring in the field. During mathematical modeling, we observed that new correlations were needed to better represent our newly adopted system.

2. Modeling Review

2.1. Models for salt dissolution in stirred tanks

[1] Aksel`rud *et al.* (1992) proposed a closed flow system, the concentration being a function of time,

$$-\frac{dm_{salt}}{dt} = k.A.(Csat - C^*) \qquad (1)$$

where m_{salt} is the mass that leaves the crystal (solid phase), t is the time, k is the mass transfer coefficient, A the total area for mass transfer, $Csat$ the concentration of the saturation point and C^* the instantaneous concentration of the solution according to time.

[3] Morse and Arvidson (2002) studied the dissolution of carbonate minerals on the surface of Earth. Their model consisted of Equation 2,

$$-\frac{dm_{calcite}}{dt} = \frac{A}{V}.k.(1-\Omega)^n \qquad (2)$$

where $m_{calcite}$ is the moles of calcite, t is the time, A is the total surface area of the solid, V is the volume of solution, k is the transfer mass coefficient, n is a positive constant expressing the order of the reaction, and Ω is the saturation state.

[4] Finneran and Morse (2009) presented a study on the calcite dissolution kinetics in saline waters based on the proposed model,

$$R = k.(1-\Omega_{calcite})^n \qquad (3)$$

where R is the dissolution rate normalized to the reaction surface area, k is the mass transfer

coefficient, $\Omega_{calcite}$ is the saturation state, and n is the reaction order.

[2] Alkattan *et al.* (1997) studied the halite dissolution kinetics considering the model of the mass coefficient according to each ion,

$$\frac{dm_{Na^+}}{dt} = \frac{dm_{Cl^-}}{dt} = k_t.(Csat - C^*) \quad (4)$$

where k_t is the mass transfer coefficient determined by the relation between the diffusion coefficient and the boundary layer coefficient,

$$k_t = \frac{D_\delta}{\delta} \quad (5)$$

In the literature, other models have been applied to study dissolution kinetics. [5] Liu and Dreybrodt (1997) studied the dissolution kinetics of calcium carbonate in aqueous solutions in turbulent flow, confirming that a diffusion boundary layer controls the dissolution.

[6] Liu *et al.* (2001) modeled the dissolution of rock salt in water. The authors found that such rocks are fractal-like and their kinetics do not adhere to classical kinetics equations, making necessary the formulation of empirical kinetics models, based on Arrhenius equation.

2.2 Literature models for estimating the convective mass transfer coefficient

One approach to determining this coefficient is to use semi-empirical correlations found in the literature. For the mass dimensionless numbers Sherwood, Schmidt and Archimedes, [7] Bird *et al.* (2001) demonstrates the following relations,

$$Sh = \frac{k.L}{D_\delta} \quad (6)$$

where Sh is the Sherwood number, k is the convective mass transfer coefficient, L is a characteristic length, and D_δ is the diffusive mass transfer coefficient.

$$Sc = \frac{\mu}{D_\delta.\rho_s} \quad (7)$$

where Sc is the Schmidt number, μ is the dynamic viscosity of the solvent, and ρ_s is the specific mass of the solvent.

$$Ar = \frac{g.L^3.\rho_s.(\rho - \rho_s)}{\mu^2} \quad (8)$$

where Ar is the Archimedes number, g is the gravity and ρ is the specific mass of the salt.

[1] Aksel`rud *et al.* 1992, observed the following relation between the dimensionless numbers,

$$Sh = 0.31.\sqrt[3]{Sc}.\sqrt[3]{Ar} \quad (9)$$

This correlation is valid only for a single type of salt, with cylindrical geometry. No information is found in his model about the influence of the degree of turbulence of the system.

The literature provides even more models to estimate the convective mass transfer coefficient. We find in [7] Bird *et al.* (2001), one model that considers the influence of the degree of turbulence through Reynolds number for a single perfect sphere particle in suspension,

$$Sh = 2 + 0.6.\sqrt[2]{Re}.\sqrt[3]{Sc} \quad (10)$$

where Re is the Reynolds number, defined as,

$$Re = \frac{dv\rho_s}{\mu} \quad (11)$$

where d is a characteristic diameter, v is the average velocity of the flow, ρ_s is the specific mass and μ is the dynamic viscosity.

2.3 Stirred tanks design.

Considering mixtures in stirred tanks, many correlations are found to estimate the variables that exist in the design of stirred tanks. [8] Nagata (1975) discussed the dimensionless numbers which are used to calculate those variables. The Reynolds number, which expresses the flow regime inside a stirred tank, is in fact a modification of Equation 11, being such,

$$Re = \frac{ND^2\rho_s}{\mu} \quad (12)$$

where N is the number of spins of the impeller per unit of time (usually in RPM, RPH, or Hz) and D is the diameter of the impeller.

Another dimensionless number important in designing stirred tanks with solids in suspension is the flux number, defined as [8] Nagata (1975),

$$N_0 = \frac{Q}{N.D^3} \quad (13)$$

where Q is the flow rate caused by the impeller. This number expresses the relation between pump forces and inertial forces.

To maintain solids in suspension it is necessary to overcome the terminal velocity of the fastest particle. The terminal velocity is the constant

velocity at which the particle decants. One method of estimating this flow rate is to conceptualize the impeller as a centrifugal pump. With due modification, this flow rate will be given by [9] SEMCO (2000),

$$Q_r = 618.{T_t}^2.F.v_t.\beta.\left[\left(6.9.\frac{H}{T_t}\right) - 0.9\right].\gamma \qquad (14)$$

$$\beta = \left(log\sqrt{f} + 0.6\right)$$

$$\gamma = (log(T_t) + 1.02)$$

where T_t is the diameter of the tank, F is a factor of homogeneity, v_t is the terminal velocity of the particle in suspension, f is the solid fraction of solids, and H is the height of fluid inside the tank. To estimate the value of F, Table 1 is found in [9] SEMCO (2000).

Table 1. Values and rules for the factor of homogeneity.

Factor *F*	Description for usage
1	Solids into motion but not suspended (deposited at the bottom)
2	Solids into motion suspended only in the bottom region of the tank
3	All solids suspended but no homogeneity
4	All solids suspended with poor homogeneity
5	All solids suspended with average homogeneity
6	All solids suspended with good homogeneity

To generate a suspension condition, the calculated flow rate must be the impellers flow rate (Q=Q_r), substituting equation 14 in 13,

$$N = 618.{T_t}^2.F.v_t.\beta.\left[\left(6.9.\frac{H}{T_t}\right) - 0.9\right].\gamma.\delta \qquad (15)$$

$$\delta = \left(\frac{1}{N_0.D^3}\right)$$

The dimensionless N_0 is found in Table 2, according to [9] SEMCO (2000); this number depends on the geometry of each type of impeller.

Table 2. Values for flux number according to the type of impeller.

Type of Impeller	N_0
PBT	0.70 – 0.90
VFBT	0.50 – 0.70
Hydrofoil HE	0.45 – 0.65
Hydrofoil LS	0.50 – 0.72
Hydrofoil HS	0.90 – 1.60
Marine Impeller (Propeller, Helix)	0.72

All presented correlations are valid only if the designed stirred tank/impeller has the geometrical dimensions inside the permitted range. Otherwise, one must look for correlations having explicit mathematical references to the geometries of the tank and impeller and the position of the impeller. Table 3 shows the conventional stirred tank design range for the geometry of the tank and impeller ([8] Nagata 1975).

Table 3. Conventional range design for stirred tanks with chicanes and propeller.

Dimension	Range accepted for Design ([8] Nagata, 1975)
D/T_t	1/4 to 1/3
H/T_t	1
C_t/T_t	1/6 to 1/2
B_W/T_t	1/12 to 1/10

D – Diameter of the impeller, T_t – Diameter of the tank, H – Liquid height inside the tank, C_t – Distance between the bottom of the tank and the impeller, B_W – width of the chicane.

3. Mathematical model proposed by this work

3.1 Proposed model for the overall mass balance between phases

The mathematical model of dissolution for the stirred tank is based on the accumulation of salt in the liquid phase. Being so, based on Equation 1 we propose the change,

$$\frac{dC}{dt} = \frac{k.A.(C^* - C)}{V} \qquad (16)$$

where C is the instantaneous concentration of salt into solution, t is the time, k is the convective mass transfer coefficient, A is the superficial area of the sample, C^* is the concentration of saturation, and V is the volume of the solution.

To define the surface area, we initially considered the particle a perfect sphere. Beginning with elementary geometry,

$$A_p = 4.\pi.\left(\frac{\overline{D_p}}{2}\right)^2 \quad (17)$$

where A_p is the surface area of the particle and D_p is the Sauter mean diameter.

The Sauter mean diameter is defined as ([10] Brennen 2005),

$$\overline{D_p} = \frac{1}{\int_0^1 \frac{dX}{D_p}} \cong \frac{1}{\sum_i \frac{\Delta X_i}{D_{pi}}} \quad (18)$$

where ΔX_i is the mass withheld in the mesh and D_{pi} is the diameter of the mesh.

For the volume of a perfect sphere we have,

$$V_p = \frac{4}{3}.\pi.\left(\frac{\overline{D_p}}{2}\right)^3 \quad (19)$$

where $V_{particle}$ is the volume of the particle.

For the specific mass we have,

$$\rho = \frac{m_p}{V_p} \quad (20)$$

where ρ is the specific mass of the salt and m_p is the mass of the particle.

Combining equations 17, 19, and 20 we may obtain an equation for the surface area of a particle which is a function of mass,

$$A_p = \pi.\left(\frac{6.m_p}{\rho.\pi}\right)^{\frac{2}{3}} \quad (21)$$

For the surface area of a population, we propose a generalization of Equation 21. Where instead of using the mass of the particle, the total mass of the population is divided by the number of particles. The result must be the average mass of a particle which belongs to that population. Multiplying that by the number of particles, the result must be the total surface area considering the average particle. Introducing a dimensionless factor which corrects the area (perfect sphere) for any geometry shape,

$$A = \frac{\pi.Np.}{\varphi}\left(\frac{6.M}{\rho.\pi.Np}\right)^{\frac{2}{3}} \quad (22)$$

where Np is the number of particles, φ is the dimensionless factor, and M is the mass of population.

For the number of particles, it is the total volume of the population divided by the average volume of one particle, after algebraic manipulation,

$$Np = \frac{6.M}{\rho.\pi.\overline{D_p}^3} \quad (23)$$

3.2 Proposed correlation for the dissolution kinetics

As soon as the mass balance equation is defined, we must decide which correlation to use to define the kinetic of dissolution, represented by variable k. Using the literature correlations presented in Section 2.2, we found none to satisfactorily represent the experimental data obtained. We understood the system in which (~~we~~) were studying the dissolution to be quite different from the classical ones observed in the literature as well as the ones in which such kinetics correlations were obtained in the past. The classical dissolution method found in the literature, often named the rotating disk method, puts one sample of perfectly defined geometry to spin in a stagnant solvent. Our system consists of a population of particles of random geometry suspended in a fluid in motion caused by an impeller. As the literature shows that the dimensionless number coefficients of mass transport are estimated based on experimental evidence, we decided to propose a more suitable correlation which may describe more efficiently the kinetics occurring in such a system.

Using the dimensionless mass transfer number, we propose:

$$Sh = a.(Re^*)^b.(Sc)^{\frac{1}{3}} \quad (24)$$

where,

$$a = (P1 + P2.(T - 318))$$

$$b = P3$$

After algebraic manipulation,

$$k = a.\left(\frac{D_\delta}{L}\right)(Re^*)^b.(Sc)^{\frac{1}{3}} \quad (25)$$

where $P1$, $P2$ and $P3$ are experimental parameters, Re^* is a modified Reynolds number, $\frac{D_\delta}{L}$ is the characteristic diffusive coefficient and Sc is the Schmidt number.

The diffusive coefficient for sodium chloride as solute and water as solvent was obtained from [11] Perry and Chilton (1980). The average coefficient at 298K is $1.44.10^{-9}$ (m^2/s). Also in [11], there is a correlation to estimate the effect of temperature over the diffusive coefficient,

$$D_\delta = \frac{\alpha.T}{\mu} \quad (26)$$

where α is a constant, estimated at a temperature of reference, this work used 298K, with a value of $4.59.10^{-15}$. D_δ is the average diffusive coefficient, μ the dynamic viscosity of the solvent and T the temperature of the solvent.

The characteristic length of the system, L, is the external diameter of the salt particle which forms the boundary layer; therefore its value comes from the granulometric analyses of the salt sample.

The modified Reynolds number is necessary due to the nature of the turbulence created in the system. Originally the degree of turbulence would be expressed by RPM. But what happens if the system changes? The degree of turbulence must, in a variable, be generalized to fit to any system. Therefore,

$$Re^* = \frac{Re - Re_c}{Re} \qquad (27)$$

where Re_c is the critical Reynolds number.

The critical Reynolds number is the minimum degree of turbulence necessary to maintain all particles in suspension. This configuration must be respected otherwise particles will be deposited in the bottom of the stirred tank, leading to a miscalculation of the total area available for mass exchange. For this work, both Re and Re_c were calculated using Equation 12. In addition, Factor 3, found in Table 1 was used to determine Re_c.

It's important to understand that both Reynolds-number forms of calculation will depend on the type of the system, mostly on the geometry of the flow.

4. Material and Methods

4.1 Characterization of the salt and solvent (mineral water)

For the experimental analysis, we obtained commercial sodium chloride to study the dissolution. The kinetics obtained here was in fact for the mixture of salts presented in each sample. Despite that, we considered the experimental result representative for the kinetics of sodium chloride only due to its high concentration, as seen in Table 4. The geometry of the particles is random and the samples were not submitted to any kind of milling. Therefore, each sample was submitted to grading analysis for characterization. Table 4 shows the typical chemical composition, provided by the manufacturer. Figure 1 shows a typical size distribution of the population of particles.

Table 4. Composition of the studied salt

Substance	Composition
$NaCl$	> 99%
KIO_3	< 1%
$Na_4Fe(CN)_6$	< 1%

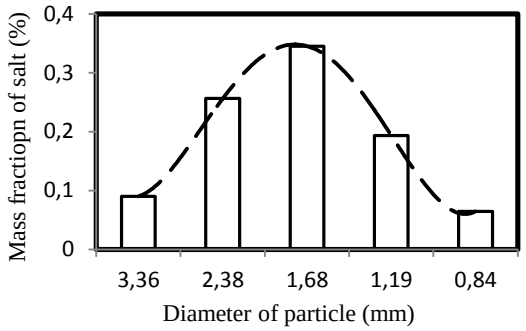

Figure 1. Typical size distribution of sample particles.

The solvent used was mineral water. Since it does not represent the water used by the industries, distilled water was not used. The chemical composition is presented in Table 5.

Table 5. Composition of the water used as solvent

Substance	Composition (mg/l)/(ppm)
$SrSO_4$	0.02
$CaSO_4$	3.40
$MgSO_4$	0.99
$Mg(HCO_3)_2$	1.46
$Mg(NO_3)_2$	0.24
KNO_3	0.33
KCl	1.09
$NaCl$	15.25
Al_2O_3	0.11

4.2 Construction of stirred tanks

To estimate the convective mass transfer coefficient, we built a stirred tank where the dissolution of the mineral salt occurred. The apparatus included a marine impeller (helix), a heater, thermometer, and metal parts for support.

The salt was organized into samples. Each sample was submitted to grading analyses, where the total mass was also obtained.

The experimental procedure was to transfer the sample to the tank, where the water was at the desired temperature and under constant agitation. At random times, samples of the solution inside the tank were taken and the final concentration of the solution measured through drying techniques. Figure 2 illustrates the experimental unit.

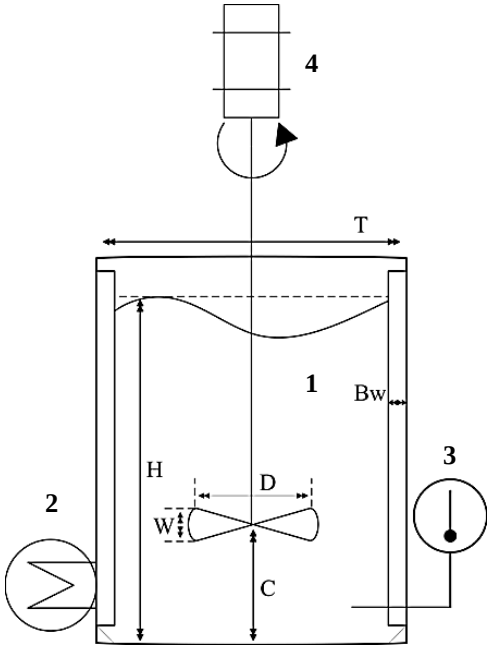

Figure 2. Stirred tank used to evaluate the dissolution of a population of salt particles.
1 – Stirred tank, 2 – Heat exchanger, 3 – Thermometer and 4 – Mechanical mixer with built in tachometer.

The dimensions of the tank are as follows in Table 3.

Table 6. Dimensions of the constructed tank

Geometrical Relations	Dimensions of this work	Dimensions range according to ([8] Nagata 1975)
D/T	1/3	1/4 to 1/3
H/T	1	1
C/T	1/3	1/6 to 1/2
B_W/T	1/10	1/12 to 1/10

4.3 Experiment design and mathematical solution

A set of experiments were done based on factor analysis. The independent variables were the Reynolds number and temperature, the dependable one being the final concentration of the solution. The initial concentration always started from zero and the volume of solvent, 4.5 liters, was the same for every experiment.

To estimate the experimental parameters in Equation 24, a nonlinear regression was used. The experimental values of the kinetic parameter k were obtained, using Equation 16, from measured values of halite concentration at the determined times. Therefore, to improve the model's capability of prediction, the nonlinear regression had to be done inside this ordinary differential equation. To do so, we coupled the least square technique with the integration of the equation. To integrate, we used a series solution. The software program Maple 14 was used as computational tool.

5. Results and Discussion

5.1 Experimental data

Figure 3 presents the results obtained for the convective mass transfer coefficient, using Equation 1. To guarantee an accurate result, each experiment was repeated three times, minimizing the experimental errors. We evaluated the replicates using the ANOVA test considering the confidence level of 95%.

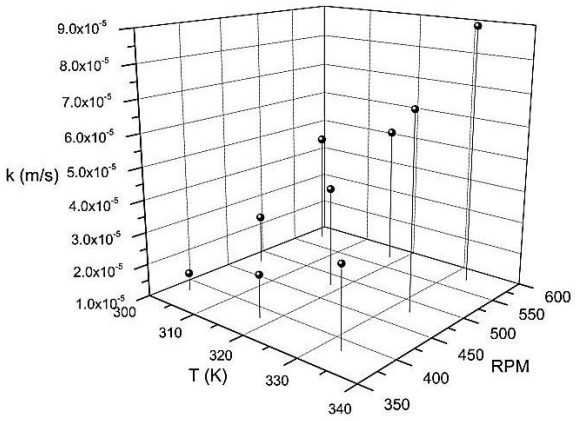

Figure 3. Observed k, varying RPM and T.

It can be observed in Figure 3 that the convective mass transfer coefficient increased as the temperature and rotation speed increased. For the temperature, the superior limit that we investigated was 333K (60^0 C); for rotation speed this limit had to be found. We believe that there is a critical point where the turbulence fails to influence the mass transfer coefficient. Observe Figure 4 for the results.

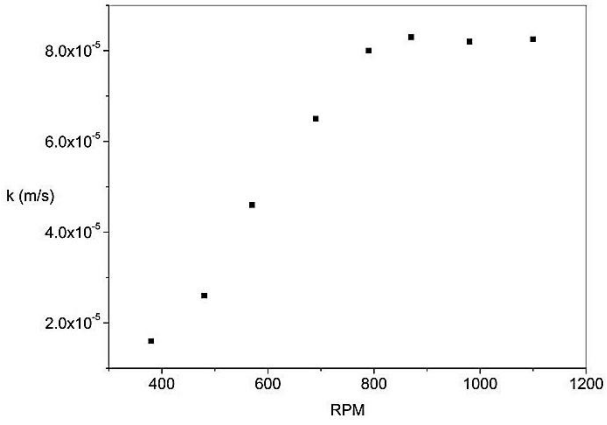

Figure 4. Observed k, varying RPM.

Figure 4 presents this critical point at approximately 900 RPM. Therefore this work is valid

between 200 RPM and 900 RPM. One must also note that this work concentrates efforts on determining a correlation which is capable of predicting the mass transfer coefficient when not only is the temperature changing, but also the region of full turbulence is not yet established.

As explained in Section 3, RPM is substituted by Re^*. Such assumption must be checked. Figure 5 proves this to be true.

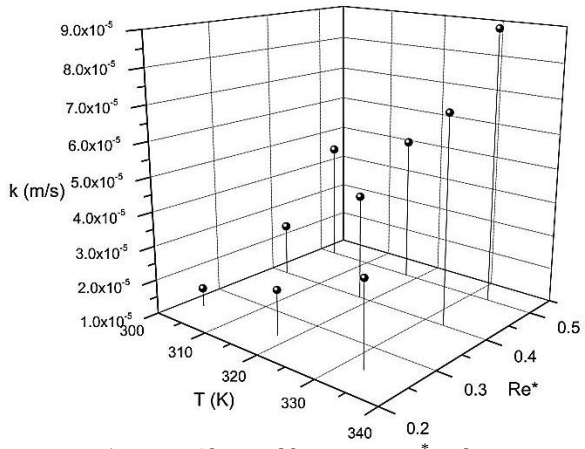

Figura 5. Observed k, varying Re^* and T

One can observe in Figure 5 that nothing has changed since the substitution of RPM per Re^*. Therefore the assumption is correct and can be used to estimate the degree of turbulence. This dimensionless number varies from 0 to 1.

5.2 Results for the proposed correlation

Having obtained the experimental data, we applied the mathematical approach explained in Section 4.3. Table 7 offers the results.

Table 7. Results obtained for the experimental parameters.

Parameter	*Value*
P1	12.79
P2	0.18
P3	1.03

5.3 Validation of the correlation proposed.

With the parameters estimated, one may solve, using any numeric method, the system model given by Equations 28; this work used a fourth order Runge-Kutta. The results of the comparison between experimental and calculated data may be seen in Figure 6.

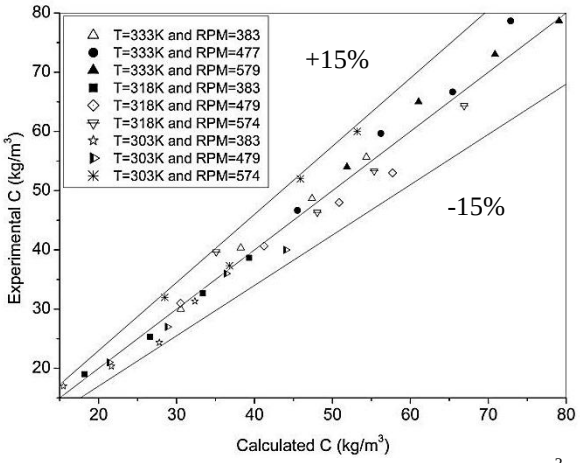

Figura 6. Experimental C versus Calculated C, in (kg/m^3).

Observing Figure 6, we affirm that the proposed correlation (Equation 24) along with the mass balance, (Equation 16) produces results with deviations of up to 15%from experimental data.

6. Conclusions

This work proposes a model to study the dissolution of sodium chloride in a non-conventional system with mineral water at transition turbulence and temperature. This work also evaluates the effects on dissolution using a population of particles to dissolve, instead of the traditional rotating disk method, being a more realistic simulation of industrial processes. We obtained a correlation capable of reproducing the experimental data with ±15% accuracy.

7. Nomenclature

Symbol	**Description**
A	Total surface area of a sample
A_p	Surface area of a particle
Ar	Archimedes number
B_w	Width of the chicane
C	Instantaneous concentration
C_t	Distance between the bottom of the tank and impeller
C^*	Concentration of saturation
D	Diameter of the impeller
d	Characteristic diameter
D_δ	Diffusive mass transfer coefficient

$\overline{D_p}$	Sauter mean diameter	m
$\overline{D_{pi}}$	Diameter of the mesh	m
F	Factor of homogeneity	*dimensionless*
f	Solid fraction of solids	*dimensionless*
g	Gravity	m/s^2
H	Liquid height inside the tank	m
k	Mass transfer coefficient	m/s
k_0	Mass transfer coefficient of reference	m/s
L	Characteristic length	m
M	Total mass of a sample	kg
m_p	Mass of a particle	kg
N	Number of rotation per unit of time	RPM
N_0	Flux number	*dimensionless*
Np	Number of particles	*dimensionless*
$P1$, $P2$, $P3$	Experimental Parameters	K^{-1}
Q	Flow rate	m^3/h
Re	Reynolds number	*dimensionless*
Re_c	Critical Reynolds number	*dimensionless*
Sc	Schmidt number	*dimensionless*
Sh	Sherwood number	*dimensionless*
T	Temperature	K
t	Time	s
T_t	Diameter of the tank	m
V	Volume of the solution	m^3
V	Velocity of the flow	m/s
V_p	Volume of a particle	m^3
v_t	Terminal velocity of the particle	m/s
ΔX_i	Mass of sample withheld in mesh	kg
ρ	Specific mass of the salt	kg/m^3
ρ_s	Specific mass of the solvent	kg/m^3
φ	Geometry factor	*dimensionless*
μ	Dynamic viscosity of the solvent	$kg/m.s$
α	Constant parameter	$m.kg/s^2.K$

8. References

[1] AKSEL'RUD, G.A, BOIKO, A.E, KASHCHEEV, A.E. *"Kinectis of the solution of mineral salts suspended in a liquid flow"*.UDC 532.73-3. SPE (Society of Petroleum Engineers).

[2] ALKATTAN M., OELKERS E.H., DANDURAND J.L., SCHOTT J., Elsevier. *"Experimental studies of halite dissolution kinetics. The effect of saturation state and the presence of trace metals"*. Chemical Geology, 137 (1997) 201-219.

[3] MORSE J.W., ARVIDSON R. S., *"The dissolution kinetics of major sedimentary carbonate minerals"*. Elsevier, Earth-science reviews 58 (2002) 51-84.

[4] FINNERAN D.W., MORSE J.W., *"Calcite dissolution kinetics in saline waters"*. Elsevier, chemical geology 268 (2009) 137-146.

[5] LIU Z., DREYBRODT W., "*Dissolution kinetics of calcium carbonate minerals in H_20-CO_2 solutions in turbulent flow: The role of diffusion boundary layer and the slow reaction $H_2O + CO_2 \leftrightarrow H^+ + HCO_3^-$*

[6] LIU C., XU L., XIAN X., "*Fractal-Like kinetics characteristics of rock salt dissolution in water". Elsevier*. Colloids and Surfaces 201 (2002) 281-285.

[7] BIRD, R.B, STEWART, W.E & LIGHTFOOT, E.N. "Transport Phenomena". Second Edition. Chemical Engineering Department. University of Wisconsin-Madison (2001).

[8] NAGATA S., "Mixing – Principles and Applications". Kodansha scientific books, 1975.

[9] SEMCO PROCESSOS, www.semcoprocessos.com.br. Accessed on 21/08/2010.

[10] BRENNEN, C. E., "Fundamentals of Multiphase flow". Cambridge University Press, 2005.

[11] PERRY, R. H. & CHILTON, H. C. Chemical Engineering Manual. Fifth edition, Guanabara Dois Editor, São Paulo: 1980.